Structure of the bottom boundary current South of Iceland and spreading of deep waters by submesoscale processes

Charly de Marez[1], Angel Ruiz-Angulo[1], and Mathieu Le Corre[2]

[1]University of Iceland
[2]SHOM

December 1, 2023

Abstract

The northeastern part of the North Atlantic subpolar gyre is a key passage for the Atlantic Meridional Overturning Circulation upper cell. To this day, the precise pathway and intensity of bottom currents in this area have not reached a consensus. In this study, we make use of regional high resolution numerical modeling to suggest that the main bottom current flowing south of Iceland originates from both the Faroe-Bank Channel and the Iceland-Faroe Ridge (with about equal contributions) and then flows along the topographic slope centered. When flowing over the rough topography, this bottom current generates a bottom mixed layer reaching 200 m height. We further demonstrate that many submesoscale structures are generated at the southernmost tip of the Icelandic shelf, thus spreading water masses in the open Iceland Basin. These findings have major implication in the better understanding of the transport of dense water masses in the North Atlantic.

Structure of the bottom boundary current South of Iceland and spreading of deep waters by submesoscale processes

Charly de Marez[1], **Angel Ruiz-Angulo**[1], **and Mathieu Le Corre** [2,3]

[1]University of Iceland, Reykjavik, Iceland
[2]Service Hydrographique et Océanographique de la Marine (SHOM), Brest, France
[3]Laboratoire d'Océanographie Physique et Spatiale (LOPS), University of Brest, CNRS, IRD, Ifremer, IUEM, France

Key Points:

- An intense bottom boundary current originating from the Iceland-Faroe Ridge and the Faroe Bank Channel flows along the Icelandic Shelf.
- The rough topography and the intensity of the current lead to bottom mixing and sustain a large bottom mixed layer.
- Subsmesoscale structures generated locally participate in the spreading of deep water masses in the Iceland Basin.

Corresponding author: Charly de Marez, `charly@hi.is`

Abstract

The northeastern part of the North Atlantic subpolar gyre is a key passage for the Atlantic Meridional Overturning Circulation upper cell. To this day, the precise pathway and intensity of bottom currents in this area have not reached a consensus. In this study, we make use of regional high resolution numerical modeling to suggest that the main bottom current flowing south of Iceland originates from both the Faroe-Bank Channel and the Iceland-Faroe Ridge (with about equal contributions) and then flows along the topographic slope centered on the 1027.75 $\mathrm{kg\,m^{-3}}$ isopycnal. When flowing over the rough topography, this bottom current generates a bottom mixed layer reaching 200 m height. We further demonstrate that many submesoscale structures are generated at the southernmost tip of the Icelandic shelf, thus spreading water masses in the open Iceland Basin. These findings have major implication in the better understanding of the transport of dense water masses in the North Atlantic, but also for the distribution of benthic species along the Icelandic shelf.

Plain Language Summary

Water masses formed in the Arctic Ocean overflow into the North Atlantic at the bottom of the ocean, forming the so-called upper cell of the Atlantic Meridional Overturning Circulation (AMOC). The pathway of the currents carrying these water masses is still under debate due to a lack of observations. In this study, we discuss in details the pathway of these bottom currents in the specific area south of Iceland. We show that a steady current flows along the Icelandic continental shelf, and then divide in smaller structures when reaching the southernmost tip of Iceland. We also show that on its way, the current mixes the bottom layer of the ocean. These findings have major implication in the understanding of heat and carbon transport at depth in this area, which constitute an important response of the climate to anthropogenic forcing.

1 Introduction

The northeastern part of the North Atlantic subpolar gyre is a key part of the Atlantic Meridional Overturning Circulation (AMOC, Buckley & Marshall, 2016). Its so-called "upper cell" ventilates the upper 2 km of the Atlantic Ocean, and it transports heat and carbon at depth from the surface (Kostov et al., 2014; Marshall et al., 2014). It therefore plays a determinant role in the response of the climate to anthropogenic forcing (Drijfhout et al., 2012; Winton et al., 2013; Meehl et al., 2014). The main sources of dense water into the upper cell are overflows from the Nordic Seas (Lozier et al., 2019; Chafik & Rossby, 2019; Tsubouchi et al., 2021). There, intense heat loss in winter transforms the water into colder and denser water masses that subsequently flow southward through gaps in topography (Brakstad, Gebbie, et al., 2023).

While it is the crossroad of this global circulation, the region south of Iceland has been poorly studied in details (see Fig. 1a for the location of the places mentioned below). At this place, there is no consensus on the shape and intensity of bottom currents. Studies agree for an overall southwestard flow from the Iceland-Faroe Ridge (IFR) and the Faroe-Bank Channel (FBC) regions toward the Iceland Basin, following the Reykjanes Ridge, see *e.g.,* Stow & Holbrook (1984); Bianchi & McCave (1999). When looking at it more precisely, opinions diverge a lot, due to the lack of available data in the area. Investigators sometimes only consider the IFR, the FBC, include an overflow over the Western Valley, or assume a pathway across the deep waters of the Iceland Basin, see *e.g.,* Bowles & Jahn (1983); Hansen (1985); Perkins et al. (1998); Hansen & Østerhus (2000, 2007); Beaird et al. (2013); Logemann et al. (2013); Guo et al. (2014); Ullgren et al. (2014); Daniault et al. (2016); Zou et al. (2017); Zhao et al. (2018); Hansen et al. (2018); Petit et al. (2019); Chafik & Rossby (2019); Semper et al. (2020); Koman et al. (2022); Brakstad, Gebbie, et al. (2023). Understanding the actual properties of local geophysical processes at depth is therefore timely. It will allow to better target future *in situ* observations aiming at quantifying water mass transport and mixing by the bottom currents, and thus better assess deep storage of anthropogenic-induced tracers.

Beyond this slowly-varying and averaged picture, it has been shown in the past years that small-scale processes have an important role in modulating the global ocean properties. This includes submesoscale balanced currents such as Submesoscale Coherent Vortices (SCVs), Intrathermocline Eddies, or fronts (McWilliams, 2019). These structures have been shown to be key for the global heat budget (Su et al., 2018) and the distribution of marine ecosystems (Lévy et al., 2018) *via* deep-reaching vertical and horizontal transports (Zhong & Bracco, 2013; Siegelman et al., 2020). Small-scale processes also include fine-scale vertical mixing, induced by deep-reaching currents and internal tides flowing over the topography (Vic et al., 2019; Gula et al., 2022; Polzin & McDougall, 2022). These processes are of major importance to regulate the transport of heat and biogeochemical tracers, and they are suggested to be a good candidate for the closing of the oceanic energy budget (Jayne, 2009; Ferrari & Wunsch, 2009; de Lavergne et al., 2022). The contribution of all these submesoscale processes in the south Icelandic dynamics has yet not been studied. However, it is likely that it plays an important role in the transport of water masses there. Note that the submesoscale is defined here as the scale at which processes happen on horizontal scales smaller than the average deformation radius (here $\mathcal{O}(20-30)$ km (LaCasce & Groeskamp, 2020)), and on vertical scales smaller than the bottom mixed layer (here $\mathcal{O}(100)$ m, see section 3.2).

In the present paper, we discuss in details the bottom circulation south of Iceland using regional high resolution numerical modeling. In particular we discuss the shape and intensity of the bottom boundary current flowing at ~ 1000 m depth along the Icelandic shelf. This current is the connection between Nordic Seas and the northeastern part of the North Atlantic subpolar gyre. In the following, mention to the "bottom boundary current" refers to this current. We further show that this latter generates numerous submesoscale features on its path and where it overshoots. This processes are shown to be of importance for the distribution of water masses in the area. In section 2 we present the methods used to investigate these processes. In section 3 we present the analysis of the numerical simulations. In section 4 we discuss and conclude on our results.

2 Methods

2.1 Numerical simulation of the North Atlantic

We use outputs of a realistic simulation of the North Atlantic Subpolar Gyre, already used and validated in previous studies, *e.g.,* Le Corre, Gula, Smilenova, & Houper (2019); Le Corre, Gula, & Treguier (2019); de Marez & Le Corre (n.d.); Smilenova et al. (n.d.); de Marez et al. (2021); Wang et al. (2022). It is performed using the Coastal and Regional Ocean COmmunity model (CROCO, Shchepetkin & McWilliams, 2005). This model solves the hydrostatic primitive equations using the full equation of state for seawater (Shchepetkin & McWilliams, 2011). The horizontal advection terms for tracers and momentum are discretized with third-order upwind advection schemes (UP3), see *e.g.* Klein et al. (2008) for a further description. This parameterization considers implicit dissipation and it damps dispersive errors.

A one-way nesting approach is used. A first simulation of the whole North Atlantic is implemented with a $\Delta x \sim 6\,\mathrm{km}$ horizontal resolution and 50 topography-following levels, such that mesoscale eddies are reasonably well resolved. It is initialized and forced at boundaries with the SODA dataset (Carton & Giese, 2008). At the surface, the forcing is obtained from the daily ERA-INTERIM dataset (Dee et al., 2011). The bathymetry is constructed from the SRTM30 PLUS dataset (Becker et al., 2009). Then, this simulation is used as boundary forcing and initialization for a second —child— simulation in the Subpolar region, with $\Delta x \sim 2\,\mathrm{km}$ horizontal resolution and 80 topography-following levels. This higher resolution resolves small scale bathymetric features. In particular, it allows an accurate description of the FBC and the IFR.

We make use of this high resolution simulation in the present study, for the period 2002-2009 (after a 2-years spin up). Reference to time averaged quantities over this period are denoted $\langle\cdot\rangle_t$. The simulation has already been thoroughly validated by Le Corre, Gula, & Treguier (2019) in the Subpolar Gyre, and at the large scale. In our domain of interest, a slight average temperature and salinity offset is seen in the whole water column (constant throughout depth). However, it does not affect the average stratification (see Fig. 2c,d) which is here the main parameter for the study of the dynamical processes. For further details, we refer the reader to Le Corre, Gula, & Treguier (2019)'s description and validation of the simulation, and their Fig. 1 that presents the simulation domain.

2.2 Particule advection simulations

We perform three offline particle advection simulations, using the velocity field from the numerical simulation on the $1027.75\,\mathrm{kg\,m^{-3}}$ isopycnal, implementing the set of python classes Parcels (Probably A Really Computationally Efficient Lagrangian Simulator). This tool has been widely used in the past few years and it is fully described in Lange & van Sebille (2017), Delandmeter & van Sebille (2019), and in references therein. The three simulations are designed such that they all are one year long. We arbitrarily chose the year 2005 of the CROCO simulation for the currents.

2.3 *in situ* data

The data used for validation and comparison was obtained from SeaDataNet and the Norwegian Marine Data Center (Brakstad, Våge, et al., 2023) for the region south-east of Iceland, corresponding to 80 CTD profiles from 1996 until 2019 covering the 4 seasons. Most of the profiles were uploaded to these open source databases by the Hydrography Observational Programme carried out by the Icelandic Marine and Freshwater Research Institute (Ólafsdóttir et al., 2020). The CTD profiles were used to validate the simulation at the virtual location of 13.7°W and 63.6°N (Stokksnes 5), shown in Fig. 1b as the point labeled 3.

3 Results

3.1 General description of the bottom current

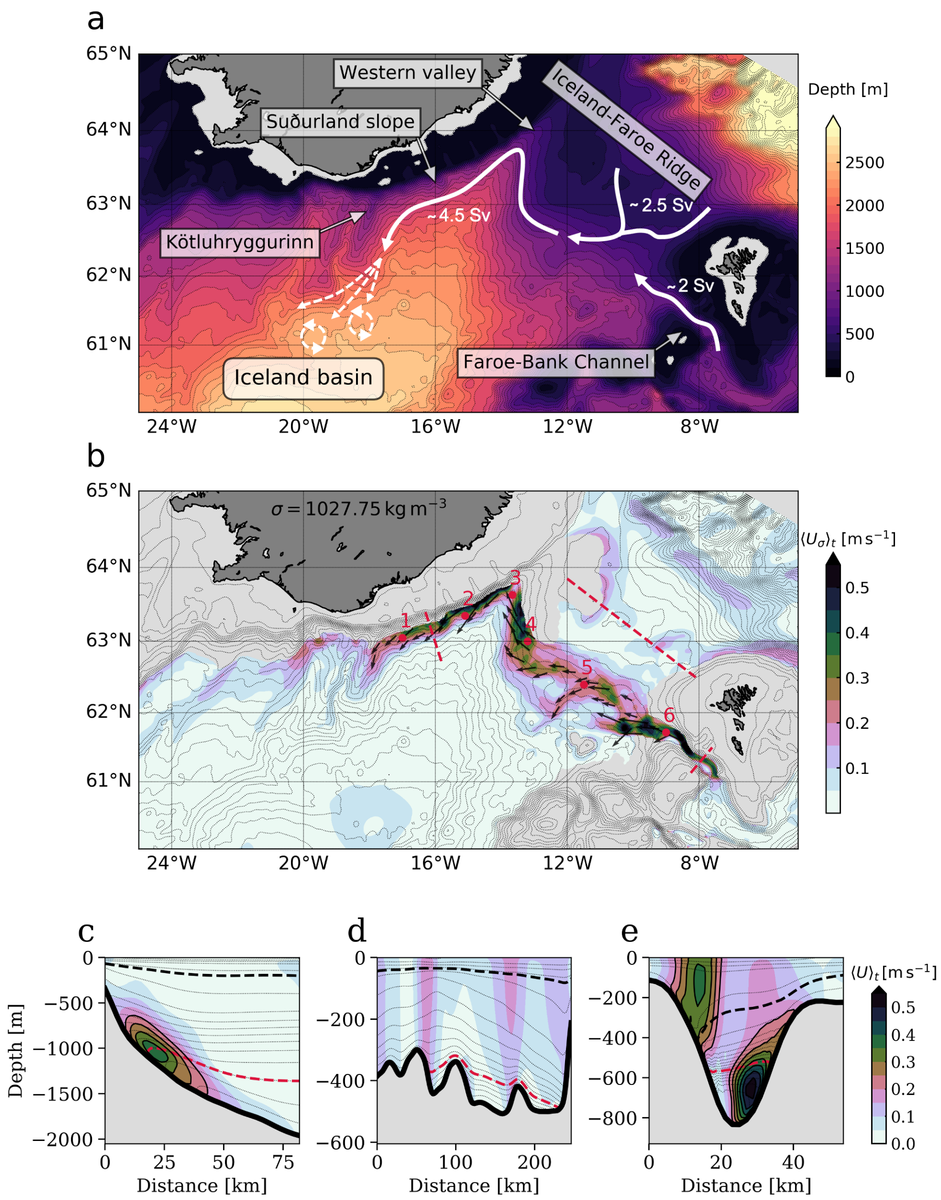

Figure 1. a: Region of interest, bathymetry, and schematic path of the bottom current; white numbers indicate the transport through the three sections shown in panels c,d,e. b: Velocity norm on the 1027.75 kg m^{-3} isopycnal; position of sections shown in panels c,d,e, position of profiles shown in Fig. 2, and bathymetry (thin black lines). c,d,e: Vertical sections of the velocity norm and isopycnals (thin dashed every 0.05 kg m^{-3}, red dashed 1027.75 kg m^{-3}, and thick dashed $\sigma_{\text{top}} = 1027.3\,\text{kg}\,\text{m}^{-3}$).

Time-averaged simulation outputs show that the bottom boundary current originates from two branches at the northeast boundary of the Iceland Basin. A first branch consists of a northwestward flow coming from the FBC. There, an intense current with average maximum velocity of 0.53 $\mathrm{m\,s^{-1}}$ located below 500 m depth flows along the northern slope of the narrow channel, see Fig. 1b,e. The transport in this channel has been shown in previous studies to be about 2 Sv (Hansen & Østerhus, 2007; Hansen et al., 2016). We determine that this transport is satisfied when integrating the crossing current between the $\sigma_{\mathrm{top}} = 1027.3\,\mathrm{kg\,m^{-3}}$ isopycnal and the bottom. A second branch consists of a southwestward flow coming from the IFR. There, two weak currents at $\sim 11°$W and $\sim 9°$W flow over the ridge. The average maximum velocity of 0.19 $\mathrm{m\,s^{-1}}$ at the bottom is seen at the western most location, see Fig. 1b,d. The crossing overflow transport between σ_{top} and the bottom is about 2.5 Sv, larger than the FBC transport because of the wider section.

When entering the Iceland Basin, the bottom boundary current stabilizes around the $1027.75\,\mathrm{kg\,m^{-3}}$ isopycnal, see Fig. 1b. It flows northward, constrained along the continental shelf. When reaching the Western Valley, it retroflects following the topography. It then flows southwestward along the continental shelf south of Iceland, namely Suðurland slope, after the name of the Icelandic southern lands. The flow is very well marked along the slope, with average maximum velocity of 0.38 $\mathrm{m\,s^{-1}}$ on the $1027.75\,\mathrm{kg\,m^{-3}}$ isopycnal, see Fig. 1c. This finding justifies the choice of this particular isopycnal for the further investigation of the current made in this study. The transport induced by the current between σ_{top} and the bottom is about 4.5 Sv, thus satisfying the mass conservation from overflows to the Suðurland slope.

Finally, the current overshoots at a submarine cape located $\sim 18°$W,62.5°N. It is called Kötluhryggurinn, "the Katla ridge", after the Katla volcano south of Iceland (Shor, 1980). A slight part of the current overflows west over Kötluhryggurinn, creating weak branches of current further west, see Fig. 1b. Further examination of the current using particle advection simulations show that these branches have few impact (section 3.3). Note that neither seasonal nor inter-annual variability of the bottom boundary current position/intensity/depth are noticed (not shown), thus justifying the use of 7-years overall time averages.

3.2 Vertical variations and mixing at the bottom

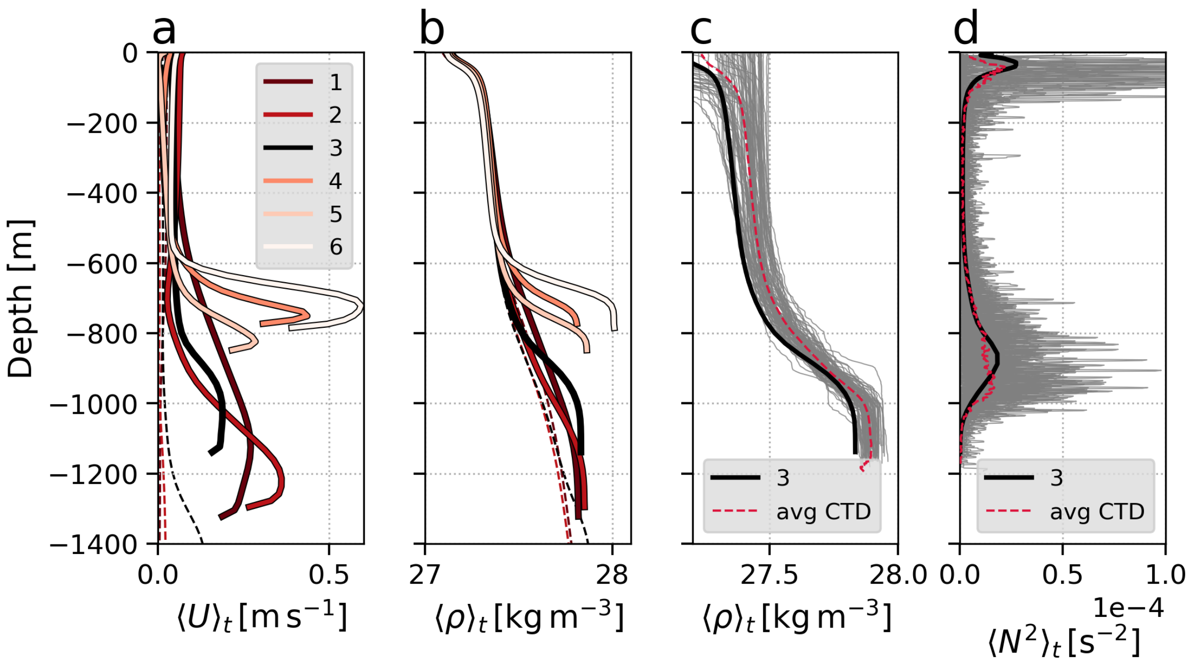

Figure 2. a (resp. b): Time-averaged velocity norm (resp. potential density) profiles at the locations shown in Fig. 1b; thin dashed profiles show profiles ∼ 50 km off-shore of the same-color profiles. c (resp. d): Comparison of potential density (resp. Brunt–Väisälä frequency) profiles between simulation (thick black) and CTD station (thin gray and thick dashed red) at location 3 (Fig. 1).

Along its path from the FBC to the Suðurland slope, the current has a Gaussian-like vertical distribution, with average maximum velocity varying between ∼0.2 and ∼0.6 $\mathrm{m\,s^{-1}}$, and average thickness varying between ∼100 m and ∼500 m, see Fig. 2a. It dives from ∼700 m depth at the FBC mouth (profile 6) to ∼1200 m depth at Kötluhryggurinn (profile 1).

A marked Bottom Mixed Layer (BML) is observed along the current path, see Fig. 2b,c,d, and is confirmed by 24 years of *in situ* data. This BML is less than 50 m thick at the FBC mouth. It then becomes thicker along the IFR reaching over 200 m in the Western Valley and along the Suðurland slope. The profile 3 position coincides with the position of CTD casts performed during a 24 years period in the Western Valley (Stokksness 5, Ólafsdóttir et al., 2020). Average vertical profile of potential density from the simulation matches with *in situ* observations. The slight offset in density is homogeneous on the vertical and is mainly due to a $\sim 0.5°$C temperature offset. Nevertheless, this does not change the dynamics as the stratification (N^2) closely matches thus proving the occurrence of this deep BML in the current path, and additionally validating one of the main feature of the simulated current.

The evolution of this BML suggest the combination of frictional and arrested bottom Ekman layers (Brink & Lentz, 2010). The FBC is a narrow-steep-smooth channel which allows the BML to be tightly confined ($\sim$ 10 km) against the slope; there, the velocity is maximum and the density contrast between the BML and the interior is also the greatest. This bottom boundary current remains confined to the slope throughout the path presented here. First evidence is that this BML is not seen $\sim$ 50 km off-shore, outside of the current path, see Fig. 2b. Along the path the BML thickness increases coincidentally with the increase in roughness on bottom topography just after the Suðurland slope, which is most likely due to submesoscale viscous processes happening at the bottom, when the current flows over the topography (Polzin et al., 2021).

3.3 The faith and spreading of carried waters

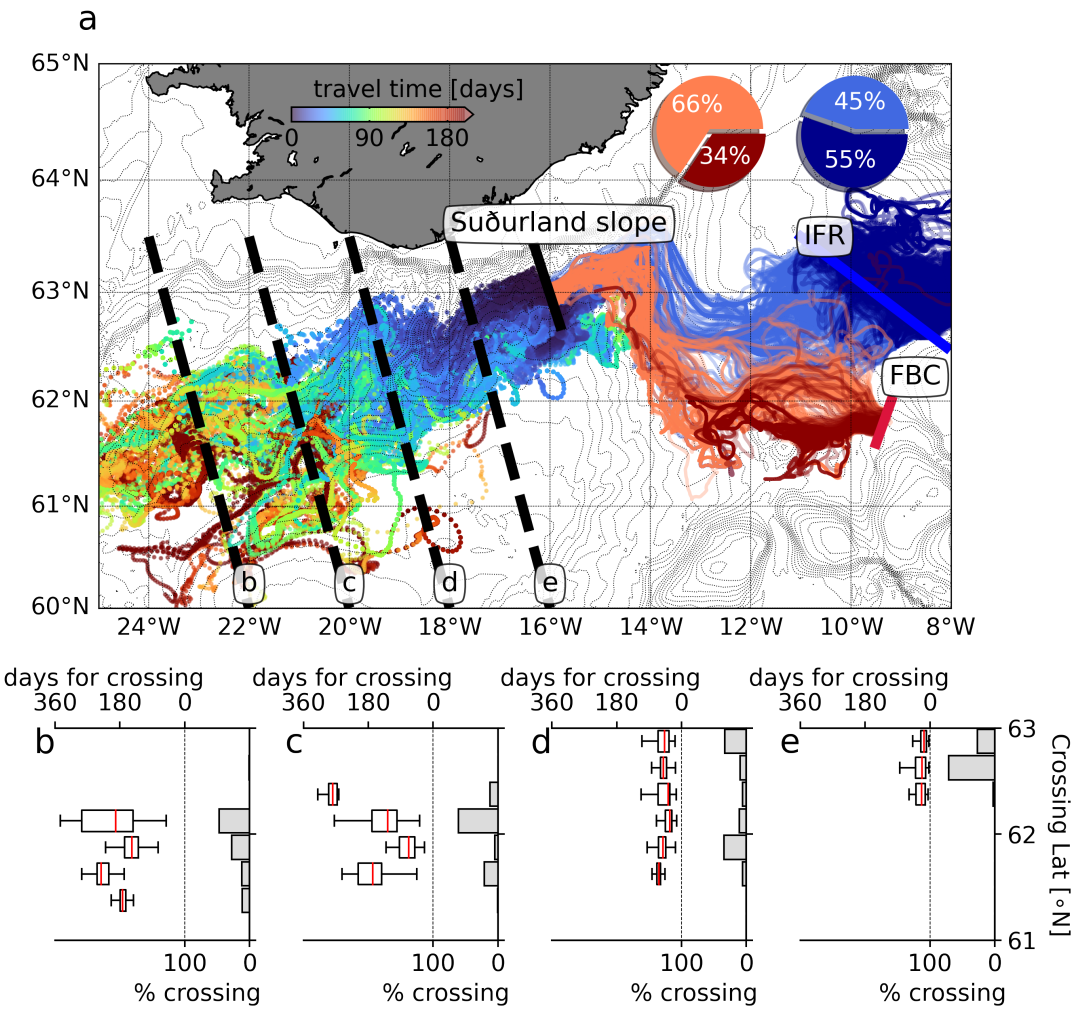

Figure 3. a: Trajectories of particles released from the IFR (blue), the FBC (red), and the Suðurland slope (rainbow color that indicates the travel time) sections; darker blue (resp. red) show trajectories of particles released from the IFR (resp. FBC) location that dit not cross the Suðurland slope section; for clarity only 1 out of 4 trajectory is shown; pie sharts indicate the percentage of trajectories that crossed the Suðurland slope section when released from either the IFR or the FBC locations; black dashed lines indicate the sections used to compute the histograms shown in bottom panels. b,c,d,e: Percentage of particles crossing the sections shown in panel a, and time for the crossing, as a function of latitude.

Two first particle advection simulations confirm that the bottom current originates from both the IFR and the FBC overflows. A total of 6 (resp. 26) particles are released everyday during 300 days along a straight line located in the FBC (resp. on the IFR) on the 1027.75 $\mathrm{kg\,m^{-3}}$ isopycnal, see Fig. 3a. Remarkably, all particles overflowing in the

Iceland Basin eventually get trapped along a very narrow path along the Suðurland slope. We then measure the number of particles from each simulation that cross a section perpendicular to the Suðurland slope, see Fig. 3a. Some particles do not reach this region at the end of the simulations (34% and 55%); those particles were either advected too slowly or flowing east of the IFR (see dark blue and dark red trajectories in Fig. 3a). Nevertheless, when particles released at both locations get trapped in the bottom current they always travel north toward the Western Valley before retroflecting to the west and crossing the Suðurland slope section. Note that an additional backward advection simulation described in Supplementary Information confirms these findings.

Then, a third simulation is designed in which 15 particles are released everyday during a year along a straight line perpendicular to the the Suðurland slope on the $1027.75\,\mathrm{kg\,m^{-3}}$ isopycnal, *i.e.,* the same section as the one mentioned previously, see Fig. 3a. Particle trajectories from this simulation shows that when reaching Kötluhryggurinn, the waters carried by the bottom current spread out in the Iceland Basin. We measure the latitude and the travel time at which particles cross four different sections, parallel to the launching section, each spaced of 2° in the longitudinal direction, see Fig. 3. Particles cross the first section (e) in a few weeks and are concentrated north of 62.5 °N, see Fig. 3e. After passing Kötluhryggurinn, and as they travel southwestward, they detach from the continental slope, and they cross sections with a large spreading, see Fig. 3b,c,d. Particles crossing section b are all located south of 62.25 °N, and some particles even crossed the 60th parallel North. The spreading is due to turbulent processes, with short time scales, as revealed by the large standard deviations of crossing times. This is also highlighted by the fact that particles are advected by a flow with high values of relative vorticity. In particular, most of the particles have a cyclonic vorticity reaching $\zeta/f > 0.5$ due to the generation of submesoscale structures at Kötluhryggurinn (see Fig. 2 of Supplementary information). These processes are described in the following section.

3.4 Submesoscale generation at Kötluhryggurinn

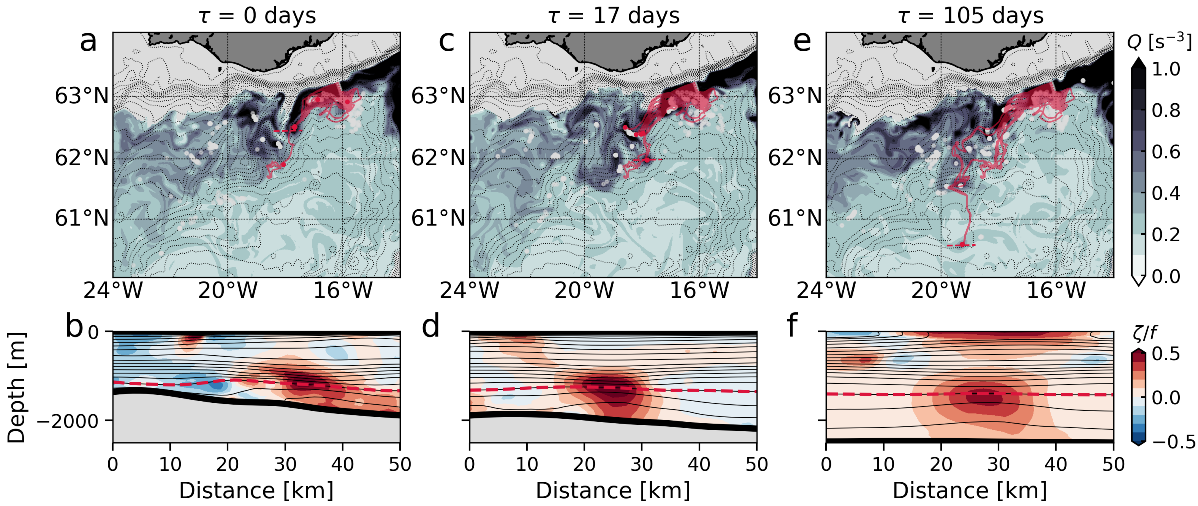

Figure 4. a,c,e: Snapshots of Potential Vorticity (divided by 10^9) on the 1027.75 $\mathrm{kg\,m^{-3}}$ isopycnal; position of particles trapped (resp. don't trapped) by the SCV at $\tau = 105$ days is shown by the red (resp. white) dots. b,d,e: vertical section of normalized relative vorticity at the position shown by the red dashed lines in top panels; isopycnals are shown in thin black lines; the 1027.75 $\mathrm{kg\,m^{-3}}$ isopycnal is shown by the thick dashed red line.

Water masses are spread out in the Iceland Basin by submesoscale structures propagating from Kötluhryggurinn. The mechanism is as follows. The bottom current flows along the Suðurland slope, concentrated around the 1027.75 $\mathrm{kg\,m^{-3}}$ isopycnal. Viscous interactions (parameterized in the model, see Le Corre, Gula, & Treguier (2019)) with the topography leads to a frictional injection of Potential Vorticity (PV) on this isopycnal. This in turn generates a change of sign of the cross-current PV gradient both horizontally and vertically (see Fig. 3 of Supplementary Information). These are the necessary conditions for Barotropic and Baroclinic instabilities to occur. This results in a highly turbulent flow along the Suðurland slope, as reflected by the high values of Eddy Kinetic Energy (EKE) and Eddy Available Potential Energy (EAPE) on this isopycnal (see Fig. 3 and 4 of Supplementary Information). The flow overshooting at Kötluhryggurinn thus does not follow the slope but meanders south in the Iceland Basin. Water masses are stirred and spread out offshore by intense fronts and rapidly varying flows with —mainly cyclonic— values of vorticity reaching $\zeta/f > 0.5$ (see Fig. 2 of Supplementary Information). Ocasionally, the tongue of potential vorticity wraps onto itself, generating cyclonic SCVs on the 1027.75 $\mathrm{kg\,m^{-3}}$ isopycnal.

The cyclonic SCVs generated at Kötluhryggurinn enhance the spreading of water masses. A particular event of SCV generation is shown in Fig. 4. This structure was generated following the mechanism discussed in the previous paragraph. It then traveled south, hundreds of kilometers, carrying water masses offshore. At $\tau = 105$ days (Fig. 4e,f), 175 particles (out of 5464 released in total during the simulation) are trapped in its core and travel southward. This represents more than 3% of the total amount of particles present along the Suðurland slope during a year, that have been spread out by this single event. Counting the number of such events is arduous because most of the time generated SCVs merge between each other making the tracking of single structures hazardous. Nevertheless, we report 15-20 events in the year 2005 of the simulation. This suggests that $\mathcal{O}(50)\%$ of water masses present along the Suðurland slope could be spread in the basin by locally generated SCVs.

4 Discussion

In this study, we investigated the bottom boundary current flowing in the north of the Iceland Basin. We showed that it originates from both the Faroe-Bank Channel and the Iceland-Faroe Ridge. It then follows the topography on the 1027.75 $\mathrm{kg\,m^{-3}}$ isopycnal where it induces bottom mixing creating a large Bottom Mixed Layer. It finally overshoots at Kötluhryggurinn, where submesoscale structures are generated and spread water masses in the open Iceland Basin.

In the past decades, circulation in the northern Iceland Basin has been investigated due to its role in the Atlantic Meridional Overturning Circulation, and numerous schematized views of the bottom circulation have emerged. The present paper aims at suggesting that the bottom circulation of the North Iceland basin is as schematized as in Fig. 1a, with a current coming from both the Faroe-Bank Channel and the Iceland-Faroe Ridge (with about equal contributions) and flowing along the topographic slope. More importantly, our study put forth the fact that when overshooting at Kötluhryggurinn, the bottom current somehow disappears and let place to a submesoscale processes-driven spreading of the water masses in the Iceland basin, thus making obsolete the view of a current steadily flowing along the Reykjanes Ridge. In particular, a significant amount of water is spread out by locally generated cyclonic SCVs. Even if only a few *in situ* experiments succeeded in measuring SCVs with a sufficient horizontal resolution (see *e.g.,* L'Hégaret et al., 2016; Meunier et al., 2018; Gula et al., 2019, and references therein), only a few observations of *cyclonic* SCVs were reported (*e.g.,* Bosse et al., 2016; de Marez et al., 2020), suggesting that anticyclonic SCVs are predominant in the deep ocean. Our findings thus further suggest that Kötluhryggurinn is an efficient generation spot for deep intense *cyclonic* SCVs. This result is to be confirmed by *in situ* measurements in the area to allow further analysis of these peculiar submesoscale structures.

The region described in this manuscript is of great importance for the future of the AMOC. Indeed, the dense water carried by the bottom current has enormous importance as it significantly contributes to the lower limb of the AMOC. Moreover, the winter convection there can create surface mixed layer depths over 700 m (Brakstad, Gebbie, et al., 2023), which in some regions allows the exchange of surface waters with dense bottom waters. The upper ocean in this region is warming up and IPCC projections suggest this will continue at even higher rates than other basins (Shu et al., 2022). South of Iceland, the combination of deep mixed layers with warmer surface waters, and thick bottom boundary currents with cold-dense waters may exchange this excess of heat resulting in changes of these dense waters in a warming climate.

The bottom boundary current described in this study also appears to be a key phenomenon to sustain biological activity in the area. Indeed, the distribution of several Cold Water Coral species, in particular *Lophelia pertusa*, strongly correlates with the position of the bottom current we described (see Fig. 4 of Buhl-Mortensen et al., 2015). It has been shown in the past that the presence of benthic species, such as Cold Water Coral, is strongly corelated to the physical and chemical properties of seawater. In particular, they rely on a renew of suspended food sources and oxygenated waters, *i.e.,* feeding currents (Mienis et al., 2019). The bottom current described here has the potential to act as a enhancement-nutrient-supply current. Its strong intensity efficiently renews the bottom water. The interaction of the current with the topography south of Iceland induces strong vertical gradients, locally enhancing vertical mixing of cold nutrient-rich bottom water to the upper layers. The bottom mixing induced by the current also enhances this water flushing, and contributes in increasing the bottom temperature, necessary condition for this species to survive. This current may have implication to a broader spectrum of benthic species, but more investigation in this direction, and a better sampling of physical-biology-related quantities at the bottom is needed to pursue this question.

Finally, even if it is mainly speculations, it is interesting to draw the question of Kötluhryggurinn formation. Studies have discussed the fact that "The Katla Ridges are smooth features with accumulation of sediment beneath the crests in excess of 1.5 kilometers. Their mode of formation is inferred to result from the rapid denudation of Iceland during the Neogene, sediment transport to the base of the slope by turbidity currents and subsequent entrainment and transport southwestward by the flow of Iceland-Scotland Overflow Water." (Shor, 1980). Even if some other exchanges from the shelf into the canyons may contribute to the sediments, several sources (see *e.g.,* Bowles & Jahn, 1983), suggest that the bottom current has lead to the formation of this bathymetric feature. Taking a step back, this suggests that the bottom current formed Kötluhryggurinn topographic anomaly, which in turn contributed to the generation of submesoscale at this particular place. This could be the signature of geological-timescale forced submesoscale process.

Acknowledgments

C.d.M. was supported by a Queen Margrethe II´s and Vigdís Finnbogadóttir's Interdisciplinary Research Centre on Ocean, Climate and Society (ROCS) postdoctoral fellowship. A.R.A. was supported by ROCS. M.L.C. was supported by the French Naval Hydrographic and Oceanographic Service (SHOM) during the writing and by UBO and Région Bretagne through ISblue, Interdisciplinary graduate school for the blue planet (ANR-17-EURE-0015) and co-funded by a grant from the French government under the program "Investissements d'Avenir" during the setup and run of the experiement. Simulations were performed using the HPC facilities DATARMOR of 'Pôle de Calcul Intensif pour la Mer' at Ifremer, Brest, France.

Open Research

CTD data were provided through SeaDataNet Pan-European infrastructure for ocean and marine data management (`https://www.seadatanet.org`), and can be downloaded as part of the SDC_ARC_DATA_TS_V2 dataset Due to the large size of simulation outputs, they are available upon request. A script to reproduce particle advection simulations can be obtained online (`https://zenodo.org/doi/10.5281/zenodo.3824499`).

References

Beaird, N., Rhines, P., & Eriksen, C. (2013). Overflow waters at the Iceland–Faroe Ridge observed in multiyear seaglider surveys. *Journal of Physical Oceanography*, *43*(11), 2334–2351.

Becker, J. J., Sandwell, D. T., Smith, W. H. F., Braud, J., Binder, B., Depner, J., ... Weatherall, P. (2009, November). Global Bathymetry and Elevation Data at 30 Arc Seconds Resolution: SRTM30_plus. *Marine Geodesy*, *32*(4), 355–371. doi: 10.1080/01490410903297766

Bianchi, G. G., & McCave, I. N. (1999). Holocene periodicity in North Atlantic climate and deep-ocean flow south of Iceland. *Nature*, *397*(6719), 515–517.

Bosse, A., Testor, P., Houpert, L., Damien, P., Prieur, L., Hayes, D., ... Mortier, L. (2016, October). Scales and dynamics of Submesoscale Coherent Vortices formed by deep convection in the northwestern Mediterranean Sea: Vortices in the NW Mediterranean Sea. *Journal of Geophysical Research: Oceans*, *121*(10), 7716–7742. doi: 10.1002/2016JC012144

Bowles, F. A., & Jahn, W. H. (1983). Geological/geophysical observations and inferred bottom-current flow: South flank Iceland—Faeroe Ridge. *Marine Geology*, *52*(3-4), 159–185.

Brakstad, A., Gebbie, G., Våge, K., Jeansson, E., & Ólafsdóttir, S. R. (2023). Formation and pathways of dense water in the Nordic Seas based on a regional inversion. *Progress in Oceanography*, *212*, 102981.

Brakstad, A., Våge, K., Ólafsdóttir, S. R., Jeansson, E., & Gebbie, G. (2023). Hydrographic and geochemical observations in the nordic seas between 1950 and 2019. , 102981. doi: 10.21335/NMDC-1271328906

Brink, K. H., & Lentz, S. J. (2010). Buoyancy arrest and bottom ekman transport. part i: Steady flow. *Journal of Physical Oceanography*, *40*(4), 621–635.

Buckley, M. W., & Marshall, J. (2016). Observations, inferences, and mechanisms of the Atlantic Meridional Overturning Circulation: A review. *Reviews of Geophysics*, *54*(1), 5–63.

Buhl-Mortensen, L., Olafsdottir, S. H., Buhl-Mortensen, P., Burgos, J. M., & Ragnarsson, S. A. (2015). Distribution of nine cold-water coral species (Scleractinia and Gorgonacea) in the cold temperate North Atlantic: effects of bathymetry and hydrography. *Hydrobiologia*, *759*, 39–61.

Carton, J. A., & Giese, B. S. (2008, August). A Reanalysis of Ocean Climate Using Simple Ocean Data Assimilation (SODA). *Monthly Weather Review*, *136*(8), 2999–3017. doi: 10.1175/2007MWR1978.1

Chafik, L., & Rossby, T. (2019). Volume, heat, and freshwater divergences in the subpolar North Atlantic suggest the Nordic Seas as key to the state of the meridional overturning circulation. *Geophysical Research Letters*, *46*(9), 4799–4808.

Daniault, N., Mercier, H., Lherminier, P., Sarafanov, A., Falina, A., Zunino, P., ... others (2016). The northern North Atlantic Ocean mean circulation in the early 21st century. *Progress in Oceanography*, *146*, 142–158.

de Lavergne, C., Groeskamp, S., Zika, J., & Johnson, H. L. (2022). The role of mixing in the large-scale ocean circulation. *Ocean mixing*, 35–63.

de Marez, C., Carton, X., Corréard, S., l'Hégaret, P., & Morvan, M. (2020). Observations of a deep submesoscale cyclonic vortex in the arabian sea. *Geophysical Research Letters*, *47*(13), e2020GL087881.

de Marez, C., Le Corre, M., & Gula, J. (2021). The influence of merger and convection on an anticyclonic eddy trapped in a bowl. *Ocean Modelling*, *167*, 101874.

Dee, D. P., Uppala, S. M., Simmons, A. J., Berrisford, P., Poli, P., Kobayashi, S., ... Vitart, F. (2011, April). The ERA-Interim reanalysis: configuration and performance of the data assimilation system. *Quarterly Journal of the Royal Meteorological Society*, *137*(656), 553–597. doi: 10.1002/qj.828

Delandmeter, P., & van Sebille, E. (2019, August). The Parcels v2.0 Lagrangian framework: new field interpolation schemes. *Geoscientific Model Development*, *12*(8), 3571–3584. doi: 10.5194/gmd-12-3571-2019

de Marez, C., & Le Corre, M. (n.d.). Can the earth be flat? A physical oceanographer's perspective.

Drijfhout, S., Van Oldenborgh, G. J., & Cimatoribus, A. (2012). Is a decline of AMOC causing the warming hole above the North Atlantic in observed and modeled warming patterns? *Journal of Climate*, *25*(24), 8373–8379.

Ferrari, R., & Wunsch, C. (2009). Ocean circulation kinetic energy: Reservoirs, sources, and sinks. *Annual Review of Fluid Mechanics*, *41*, 253–282.

Gula, J., Blacic, T. M., & Todd, R. E. (2019, March). Submesoscale Coherent Vortices in the Gulf Stream. *Geophysical Research Letters*, *46*(5), 2704–2714. doi: 10.1029/2019GL081919

Gula, J., Taylor, J., Shcherbina, A., & Mahadevan, A. (2022). Submesoscale processes and mixing. In *Ocean mixing* (pp. 181–214). Elsevier.

Guo, C., Ilicak, M., Fer, I., Darelius, E., & Bentsen, M. (2014). Baroclinic instability of the Faroe Bank Channel overflow. *Journal of Physical Oceanography*, *44*(10), 2698–2717.

Hansen, B. (1985). The circulation of the northern part of the Northeast Atlantic. *Rit. Fisk.*, *9*, 110–126.

Hansen, B., Húsgarð Larsen, K. M., Hátún, H., & Østerhus, S. (2016). A stable faroe bank channel overflow 1995–2015. *Ocean Science*, *12*(6), 1205–1220.

Hansen, B., Larsen, K. M. H., Olsen, S. M., Quadfasel, D., Jochumsen, K., & Østerhus, S. (2018). Overflow of cold water across the Iceland–Farœ Ridge through the Western Valley. *Ocean Science*, *14*(4), 871–885.

Hansen, B., & Østerhus, S. (2000). North atlantic–nordic seas exchanges. *Progress in oceanography*, *45*(2), 109–208.

Hansen, B., & Østerhus, S. (2007). Faroe bank channel overflow 1995–2005. *Progress in Oceanography*, *75*(4), 817–856.

Jayne, S. R. (2009). The impact of abyssal mixing parameterizations in an ocean general circulation model. *Journal of Physical Oceanography*, *39*(7), 1756–1775.

Klein, P., Hua, B. L., Lapeyre, G., Capet, X., Le Gentil, S., & Sasaki, H. (2008, August). Upper Ocean Turbulence from High-Resolution 3D Simulations. *Journal of Physical Oceanography*, *38*(8), 1748–1763.

Koman, G., Johns, W., Houk, A., Houpert, L., & Li, F. (2022). Circulation and overturning in the eastern North Atlantic subpolar gyre. *Progress in oceanography*, *208*, 102884.

Kostov, Y., Armour, K. C., & Marshall, J. (2014). Impact of the Atlantic meridional overturning circulation on ocean heat storage and transient climate change. *Geophysical Research Letters*, *41*(6), 2108–2116.

LaCasce, J. H., & Groeskamp, S. (2020). Baroclinic modes over rough bathymetry and the surface deformation radius. *Journal of Physical Oceanography*, *50*(10), 2835–2847.

Lange, M., & van Sebille, E. (2017, November). Parcels v0.9: prototyping a Lagrangian ocean analysis framework for the petascale age. *Geoscientific Model Development*, *10*(11), 4175–4186. doi: 10.5194/gmd-10-4175-2017

Le Corre, M., Gula, J., Smilenova, A., & Houper, L. (2019). On the dynamics of a deep quasi-permanent anticylonic eddy in the rockall trough. *French Congress of Mechanics*.

Le Corre, M., Gula, J., & Treguier, A. M. (2019). Barotropic vorticity balance of the north atlantic subpolar gyre in an eddy-resolving model. *Ocean Science*. doi: 10.5194/os-2019-114

Lévy, M., Franks, P. J., & Smith, K. S. (2018). The role of submesoscale currents in structuring marine ecosystems. *Nature communications*, *9*(1), 4758.

L'Hégaret, P., Carton, X., Louazel, S., & Boutin, G. (2016, May). Mesoscale eddies and submesoscale structures of Persian Gulf Water off the Omani coast in spring 2011. *Ocean Science*, *12*(3), 687–701. doi: 10.5194/os-12-687-2016

Logemann, K., Ólafsson, J., Snorrason, Á., Valdimarsson, H., & Marteinsdóttir, G. (2013). The circulation of icelandic waters–a modelling study. *Ocean Science*, *9*(5), 931–955.

Lozier, M. S., Li, F., Bacon, S., Bahr, F., Bower, A. S., Cunningham, S., ... others (2019). A sea change in our view of overturning in the subpolar North Atlantic. *Science*, *363*(6426), 516–521.

Marshall, J., Armour, K. C., Scott, J. R., Kostov, Y., Hausmann, U., Ferreira, D., ... Bitz, C. M. (2014). The ocean's role in polar climate change: asymmetric arctic and antarctic responses to greenhouse gas and ozone forcing. *Philosophical Transactions of the Royal Society A: Mathematical, Physical and Engineering Sciences*, *372*(2019), 20130040.

McWilliams, J. C. (2019, December). A survey of submesoscale currents. *Geoscience Letters*, *6*(1). doi: 10.1186/s40562-019-0133-3

Meehl, G. A., Goddard, L., Boer, G., Burgman, R., Branstator, G., Cassou, C., ... others (2014). Decadal climate prediction: an update from the trenches. *Bulletin of the American Meteorological Society*, *95*(2), 243–267.

Meunier, T., Tenreiro, M., Pallàs-Sanz, E., Ochoa, J., Ruiz-Angulo, A., Portela, E., ... Carton, X. (2018, August). Intrathermocline Eddies Embedded Within an Anticyclonic Vortex Ring. *Geophysical Research Letters*, *45*(15), 7624–7633. doi: 10.1029/2018GL077527

Mienis, F., Bouma, T., Witbaard, R., Van Oevelen, D., & Duineveld, G. (2019). Experimental assessment of the effects of coldwater coral patches on water flow. *Ma-*

rine Ecology Progress Series, *609*, 101–117.

Ólafsdóttir, S. R., Danielsen, M., Ólafsdóttir, E., Benoit-Cattin, A., Sliwinski, J., & Macrander, A. (2020). Ástand sjávar 2017 og 2018. *Haf-og vatnarannsóknir*.

Perkins, H., Hopkins, T., Malmberg, S.-A., Poulain, P.-M., & Warn-Varnas, A. (1998). Oceanographic conditions east of Iceland. *Journal of Geophysical Research: Oceans*, *103*(C10), 21531–21542.

Petit, T., Mercier, H., & Thierry, V. (2019). New insight into the formation and evolution of the East Reykjanes Ridge current and Irminger current. *Journal of Geophysical Research: Oceans*, *124*(12), 9171–9189.

Polzin, K. L., & McDougall, T. J. (2022). Mixing at the ocean's bottom boundary. In *Ocean mixing* (pp. 145–180). Elsevier.

Polzin, K. L., Wang, B., Wang, Z., Thwaites, F., & Williams III, A. J. (2021). Moored flux and dissipation estimates from the northern deepwater gulf of mexico. *Fluids*, *6*(7), 237.

Semper, S., Pickart, R. S., Våge, K., Larsen, K. M. H., Hátún, H., & Hansen, B. (2020). The Iceland-Faroe Slope Jet: a conduit for dense water toward the Faroe Bank Channel overflow. *Nature communications*, *11*(1), 5390.

Shchepetkin, A. F., & McWilliams, J. C. (2005, January). The regional oceanic modeling system (ROMS): a split-explicit, free-surface, topography-following-coordinate oceanic model. *Ocean Modelling*, *9*(4), 347–404.

Shchepetkin, A. F., & McWilliams, J. C. (2011, January). Accurate Boussinesq oceanic modeling with a practical, "Stiffened" Equation of State. *Ocean Modelling*, *38*(1-2), 41–70. doi: 10.1016/j.ocemod.2011.01.010

Shor, A. N. (1980). *Bottom currents and abyssal sedimentation processes south of iceland* (Doctoral dissertation, Massachusetts Institute of Technology). Retrieved from `https://dspace.mit.edu/handle/1721.1/58122`

Shu, Q., Wang, Q., Årthun, M., Wang, S., Song, Z., Zhang, M., & Qiao, F. (2022). Arctic ocean amplification in a warming climate in cmip6 models. *Science Advances*, *8*(30), eabn9755.

Siegelman, L., Klein, P., Rivière, P., Thompson, A. F., Torres, H. S., Flexas, M., & Menemenlis, D. (2020). Enhanced upward heat transport at deep submesoscale ocean fronts. *Nature Geoscience*, *13*(1), 50–55.

Smilenova, A., Gula, J., Le Corre, M., Houpert, L., & Reecht, Y. (n.d.). A persistent deep anticyclonic vortex in the rockall trough sustained by anticyclonic vortices shed from the slope current and wintertime convection.

Stow, D., & Holbrook, J. (1984). North Atlantic contourites: an overview. *Geological Society, London, Special Publications*, *15*(1), 245–256.

Su, Z., Wang, J., Klein, P., Thompson, A. F., & Menemenlis, D. (2018). Ocean submesoscales as a key component of the global heat budget. *Nature communications*, *9*(1), 775.

Tsubouchi, T., Våge, K., Hansen, B., Larsen, K. M. H., Østerhus, S., Johnson, C., … Valdimarsson, H. (2021). Increased ocean heat transport into the Nordic Seas and Arctic Ocean over the period 1993–2016. *Nature Climate Change*, *11*(1), 21–26.

Ullgren, J. E., Fer, I., Darelius, E., & Beaird, N. (2014). Interaction of the Faroe Bank Channel overflow with Iceland Basin intermediate waters. *Journal of Geophysical Research: Oceans*, *119*(1), 228–240.

Vic, C., Naveira Garabato, A. C., Green, J. M., Waterhouse, A. F., Zhao, Z., Melet, A., … Stephenson, G. R. (2019). Deep-ocean mixing driven by small-scale internal tides. *Nature communications*, *10*(1), 2099.

Wang, L., Gula, J., Collin, J., & Mémery, L. (2022). Effects of Mesoscale Dynamics on the Path of Fast-Sinking Particles to the Deep Ocean: A Modeling Study. *Journal Of Geophysical Research-oceans*, *127*(7).

Winton, M., Griffies, S. M., Samuels, B. L., Sarmiento, J. L., & Frölicher, T. L. (2013). Connecting changing ocean circulation with changing climate. *Journal of climate*, *26*(7), 2268–2278.

Zhao, J., Bower, A., Yang, J., Lin, X., & Penny Holliday, N. (2018). Meridional heat transport variability induced by mesoscale processes in the subpolar North Atlantic. *Nature communications*, *9*(1), 1124.

Zhong, Y., & Bracco, A. (2013). Submesoscale impacts on horizontal and vertical transport in the gulf of mexico. *Journal of Geophysical Research: Oceans*, *118*(10), 5651–5668.

Zou, S., Lozier, S., Zenk, W., Bower, A., & Johns, W. (2017). Observed and modeled pathways of the Iceland Scotland Overflow Water in the eastern North Atlantic. *Progress in Oceanography*, *159*, 211–222.

Supporting Information for "Structure of the bottom boundary current South of Iceland and spreading of deep waters by submesoscale processes"

Charly de Marez[1], **Angel Ruiz-Angulo**[1], **and Mathieu Le Corre** [2,3]

[1]University of Iceland, Reykjavik, Iceland

[2]Service Hydrographique et Océanographique de la Marine (SHOM), Brest, France

[3]Laboratoire d'Océanographie Physique et Spatiale (LOPS), University of Brest, CNRS, IRD, Ifremer, IUEM, France

1 Backward particule advection simulation

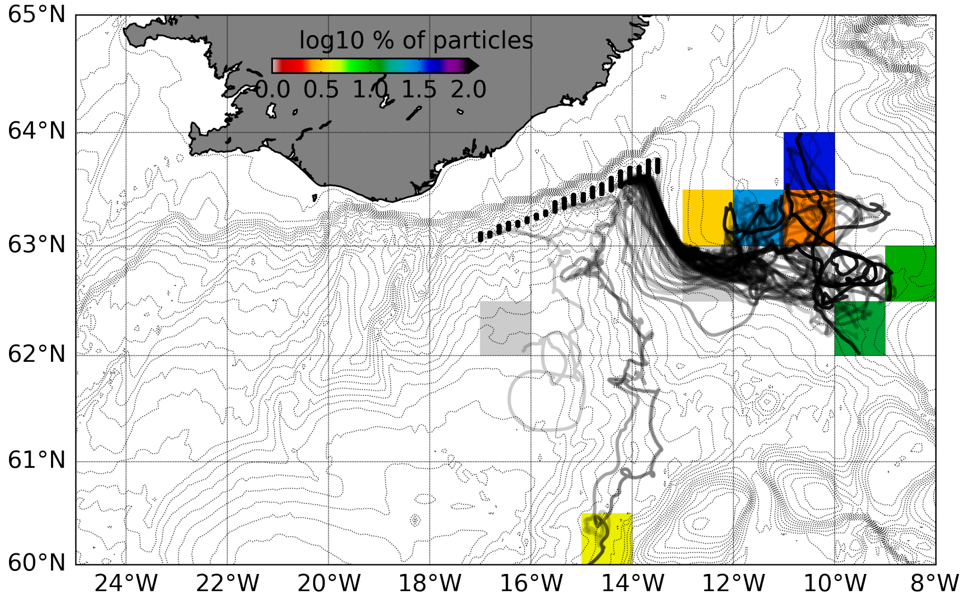

Figure 1. Distribution of the particle origin position from backward Lagrangian simulation (only the 3,342 particles that have traveled more than 300 km are considered); the release position of particles is shown by the black dots.

Corresponding author: Charly de Marez, `charly@hi.is`

We performed a backward advection simulation. We released 75 particles along the Suðurland slope every days of year 2005 on the 1027.75 $\mathrm{kg\,m^{-3}}$ isopycnal, and advect them backward to locate their origin. We only considered particles that have traveled more than 200 km (a large number of particles are discarded as they got trapped on the edge of the isopycnal and stopped moving). Most of the remaining particles originate from the mouth of the Faroe Bank Channel and the Iceland-Faroe Ridge, as suggested by the average velocity norm from simulations, and the 2 forward particle advection simulation discussed in the main manuscript. We can roughly estimate that $\mathcal{O}(10)$ % particles come from the FBC mouth, and that $\mathcal{O}(50)$ % particles come from the IFR. These are only estimates. An accurate estimation could be done using a 3D particle advection using the full (3D) velocity field, but it is not the topic of the current study.

This simulations also highlights the fact that a few particles ($< 5\%$) may end up along the slope in the bottom boundary current while traveling from the interior (or the East) of the Iceland Basin. This is mostly due to the intense deep-reaching mesoscale turbulent flow in the Iceland Basin that stir the deep water masses, and thus contributes in bringing waters in the bottom boundary current.

2 Vorticity of advected particules

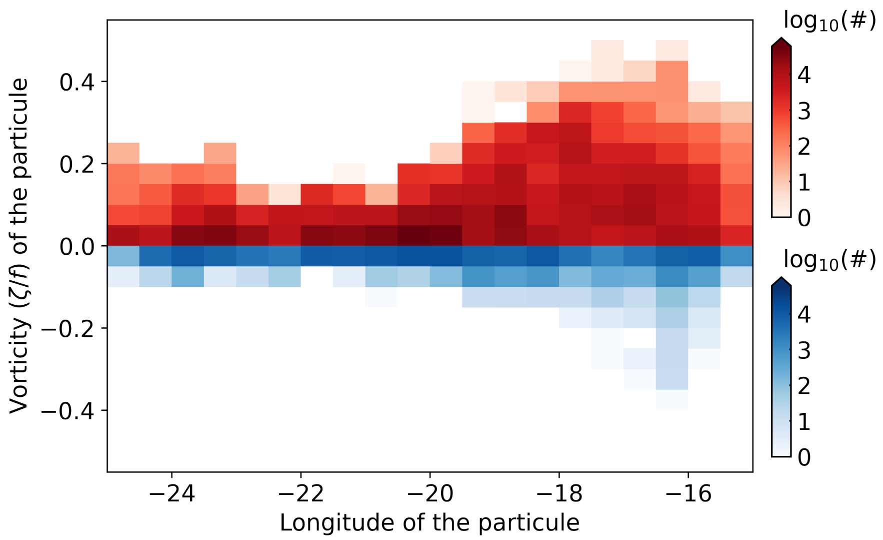

Figure 2. Vorticity histogram of particles released along the Suðurland slope as a function of the longitude of the particle. Red (resp. blue) bins show the number of particles with cyclonic (resp. anticyclonic) vorticity. To compute the histogram, all timesteps are considered.

3 Cross-slope condition for geophysical instability

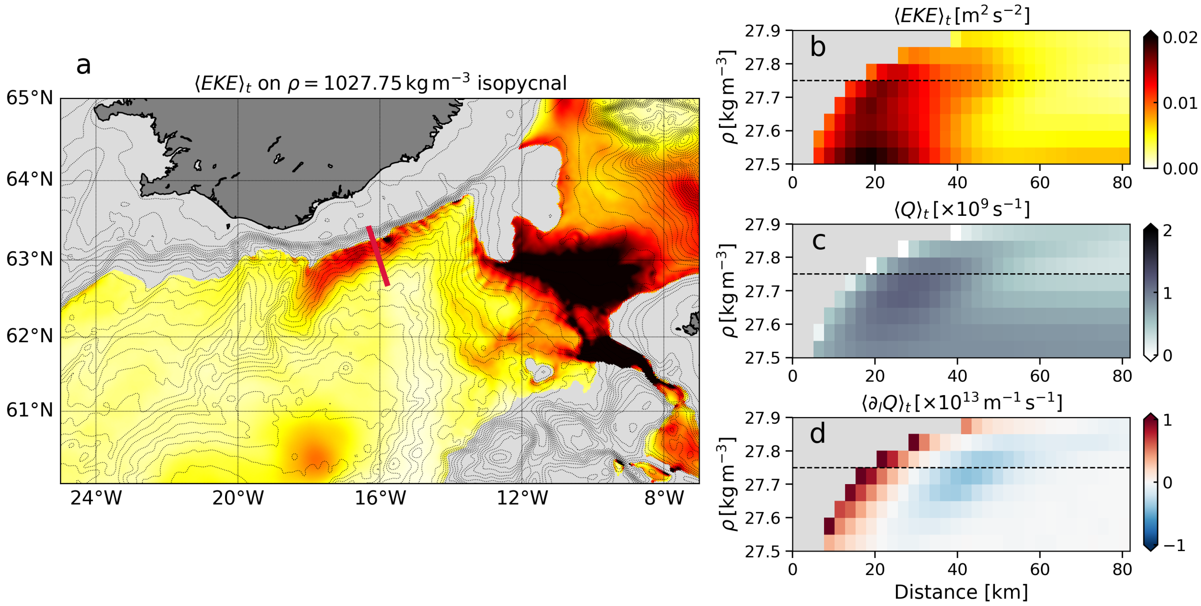

Figure 3. a. Mean EKE on the 1027.75 kg m^{-3} isopycnal. b,c,d, sections of mean EKE, PV, and cross-slope gradient of PV along the line shown in a; sections are shown in isopycnal coordinates.

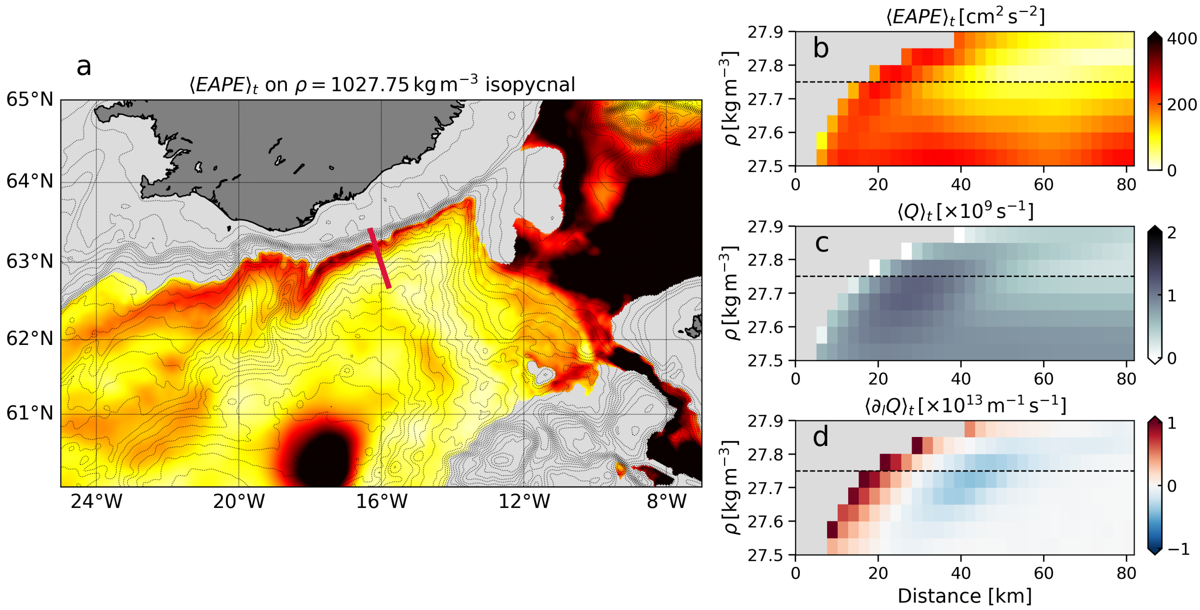

Figure 4. Same as Fig. 3, but with panels a,b showing the EAPE.